ARCHIVES OF ACOUSTICS
9, 1-2, 41-50 (1984)

ESTIMATION OF CALCIFICATION DETECTABILITY IN BREAST TISSUES BY MEANS OF THE ULTRASONIC ECHO AND SHADOW METHODS

L. FILIPCZYŃSKI, G. ŁYPACEWICZ

Department of Ultrasound, Institute of Fundamental Technological Research, Polish Academy of Sciences
(00-049 Warsaw, ul. Świętokrzyska 21 Poland,)

Microcalcifications originate at an early stage of the breast cancer. Assuming their mechanical properties to be similar to those of the bone tissue, analysis was performed to find the smallest calcification size to be determined with ultrasonic echo and shadow methods. Taking into account the tissue interference background which has been determined experimentally, the electrical properties of the ultrasonograph and attenuation loss, basing on the theory of reflection from rigid and elastic spheres, the theoretical detectivity of calcifications in breasts could be estimated. It has been shown that at a frequency of 3 MHz spherical calcifications with the radii $a > 0{,}15$ mm situated at the depth $R = 4$ cm may be theoretically detected when using the echo method and a linear receiver.

With the shadow method calcifications with radii greater than $a = 1.5$ mm are estimated to be detectable. This could be shown theoretically and experimentally using spheres made of plasticine.

1. Introduction

The ultrasonic method is one of the more recent ways of detecting breast tumors [7]. The reactions which proceed in breast tissue cells and which cause calcifications when the cancer occurs are present at a very early stage of its development. They usually occur prior to the infiltration phase, which is visible in a mammogram or an X-ray microgram preparation [8]. In view of this, the question arrises as to what are the possibilities of detecting small calcifications by the ultrasonic method. This paper presents an attempt to explain the problem and to estimate the minimum calcification size which can be detected by the ultrasonic echo and shadow methods.

2. Assumptions of the analysis

It is assumed that the acoustic parameters of calcifications are the same as those of the bone tissue [11]; the longitudinal wave velocity $c_L = 3.2$ km/s, the density $\varrho = 2.23$ g/cm^3. As we do not have any information regarding the transverse wave velocity c_T, the Poisson ratio ν will be assumed in computations as a parameter. It is assumed that the calcification has the shape and properties of elastic and rigid spheres placed in a fluid medium (soft tissue).

3. Reflexion from the sphere

If $\lambda \ll a$, then the power contained in an area πa^2 of the incident beam is equal to the power reflected equally in all directions from a rigid sphere [9]. With p_0 denoting the acoustic pressure amplitude of the plane incident wave, ϱc the acoustic impedance of the soft tissue, we obtain at the distance $r \gg a$:

$$\pi a^2 p_0^2/2\varrho c = 4\pi r^2 p_s^2/2\varrho c, \tag{1}$$

or

$$p_s = p_0 \frac{a}{2r} f_\infty(ka) \tag{2}$$

where p_s denotes the acoustic pressure amplitude of the scattered wave, $f_\infty(ka)$ the far field form function. For a rigid sphere when $\lambda \ll a$ the function $f_\infty(ka) \to 1$; for an elastic sphere it depends on the elastic properties of the sphere, that of the surrounding medium, on the wavelength and on the sphere radius.

To determine the far field form function $f_\infty(ka)$ for the parameters of calcifications given above, a computer program was elaborated with different values of the Poisson ratio ν on the basis of the theory given by several authors [1, 5, 6]. Fig. 1 shows the results obtained [2]. It follows from these curves that the function $f_\infty(ka)$ does not depend on ν until the value $ka < 1.5$. Considering the Poisson ratio for various solids [2], it seems to us that for calcifications the value $\nu \approx 0.2$ may be assumed for the interval $ka = 1.5 \div 3$. For $ka > 3$ the far field form function $f_\infty(ka)$ shows many peaks which correspond to many resonances occurring in the sphere. FLAX *et al.* [3] has shown that in this case the scattering is the superposition of wave scattering by a rigid sphere and a number of resonances arising in the sphere. These resonances differ in character, since they correspond to different wave types, including, for example, also surface waves, of the "whispering gallery" type and so on.

Therefore, in the case of calcifications with irregular shapes and corrugated surfaces, one should expect that a number of resonances will not occur at all and the function $f_\infty(ka)$ will come closer to the curve for a rigid sphere. Thus we assume $f_\infty(ka) \approx 1$ for $ka > 3$ [2].

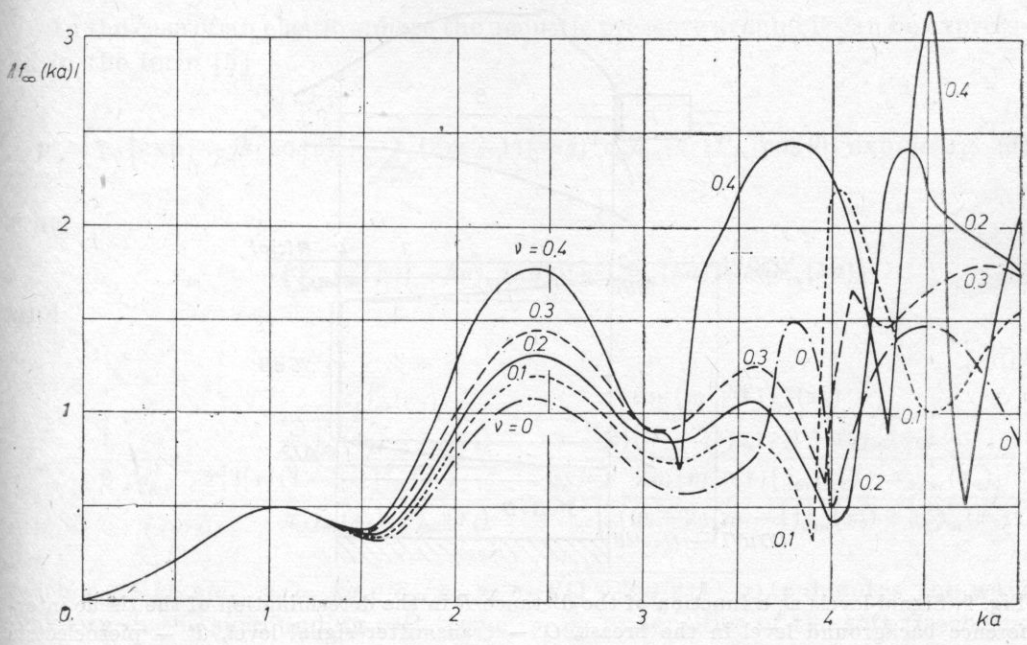

Fig. 1. The far field form function $f_\infty(ka)$ computed for an elastic spherical calcification model with various Poisson ratios ν

4. Detectability of calcifications with the echo method

For quantitative estimation of the detectability we assume the following typical parameters of the ultrasonograph [2]: sensitivity 10 μV, transmitter voltage (in pulse) 250 V, frequency 3 MHz, piezoelectric transducing losses — 15 dB, attenuation in breast tissue — 1.1 dB/MHz cm. Many echoes obtained at the boundaries of fat, fibre and gland tissues and on their inhomogeneities form a tissue interference background whose level is much higher than the electronic noise level of the ultrasonograph.

To determine this tissue interference background level, measurements were performed in the normal breasts of 30 women 25-45 years old by means of a USK 79/M ultrasonocardiograph [2] (frequency 3 MHz, transducer diameter 15 mm, weak focusing beam). The level of the tissue interference background was found to be $D = 31 \pm 4$ dB (in small breasts) and 49 dB (in large breasts) higher than the electronic noise level of the ultrasonocardiograph at a depth of 4 cm (Fig. 2). Taking into consideration the electronic noise level $N = -148$ dB (in respect to the transmitter voltage level), the value of D, piezoelectric transducing losses T, attenuation losses A, one obtains the remaining value of the electrical dynamics W for the ratio p_s/p_0. Hence from formula (2) one determines the product $ka = 1.9$ ($a = 0.15$ mm), of the sphere-shaped calcification which gives (in large breasts) an echo at the level of the tissue interference background $N + D$, at the depth $R = 4$ cm.

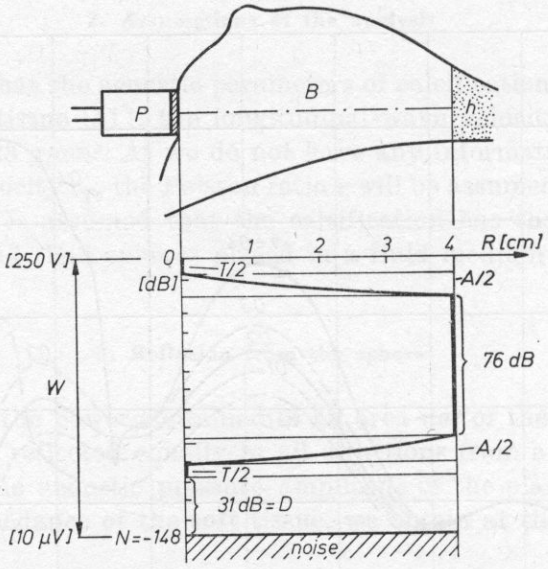

Fig. 2. Signal levels as a function of the distance R in the determination of the tissue interference background level in the breast, O — transmitter signal level, T — piezoelectric transducing losses, A — attenuation losses, N — electronic noise level, D — experimentally determined level increase due to the tissue interference background, W — electrical dynamics of the ultrasonograph, h — hypothetic tissue reflector, P — ultrasonic probe, B — breast

5. The shadow method

In this method one observes instead of the echo a shadow which occurs behind the calcification. It arises against the white background of many small echoes caused by the waves which are scattered by tissue inhomogeneities. Let us assume a rigid sphere as the model of the calcification. The acoustic field around the sphere can be expressed in the form [10],

$$p = p_0 \left\{ \exp(jkr\cos\vartheta) - \sum_{m=0}^{\infty} j^m (2m+1) \frac{j'_m(ka)}{h'_m(ka)} P_m(\cos\vartheta) h_m(kr) \right\} \exp(j\omega t), \quad (3)$$

where p denotes the acoustic pressure around the sphere, $k = 2\pi/\lambda$, $P_m(\cos\vartheta)$ — a Legendre polynomial, ϑ — the angle between the direction of the incident wave and the direction under consideration, h_m and h'_m — a spherical Hankel function of the second kind and its derivative, j' — a derivative of the spherical Bessel function, m — a natural number, $j = \sqrt{-1}$, ω — pulsation, t — time. To determine the shadow behind the rigid sphere from expression (3) a computer program was elaborated and the results are presented in Fig. 3. They show that the shadow starts forming when $ka = 10$; if $ka = 15$ the shadow becomes better visible; for $ka = 20$ and 25 it is very distinct.

In the case of an elastic sphere the acoustic pressure around it can be expressed in the form [5]

$$p = p_0\left\{\exp(-jkr\cos\theta) + \sum_{m=0}^{\infty}(2m+1)(-j)^m c_m h_m(kr) P_m(\cos\theta)\right\}\exp(j\omega t), \quad (4)$$

where

$$c_m = -[F_m j_m(ka) - ka j_m'(ka)]/[F_m h_m(ka) - ka h_m'(ka)] \quad (5)$$

and

$$F_m = \frac{1}{2}\frac{\varrho}{\varrho_s}x_2^2 \frac{\dfrac{x_1 j_m'(x_1)}{x_1 j_m'(x_1) - j_m(x_1)} - \dfrac{2m(m+1)j_m(x_2)}{(m+2)(m-1)j_m(x_2) + x_2^2 j_m''(x_2)}}{\dfrac{x_1^2\{[\nu/(1-2\nu)]j_m(x_1) - j_m''(x_1)\}}{x_1 j_m'(x_1) - j_m(x_1)} - \dfrac{2m(m+1)[j_m(x_2) - x_2 j_m'(x_2)}{(m+2)(m-1)j_m(x_2) + x_2^2 j_m''(x_2)}}, \quad (6)$$

with $x_1 = ka\ c/c_L$, $x_2 = ka\ c/c_T$, $c_T = c_L\sqrt{(1-2\nu)/2(1-\nu)}$. c denotes the wave velocity in the surrounding soft tissue, ϱ, ϱ_s — densities of the soft tissue and the sphere, respectively, θ — the angle between the shadow axis and the direction under consideration. Fig. 4 shows angular distributions of the acoustic pressure amplitude computed from formulae ((4), (5), (6)) for various values of ka, when $\nu = 0.2$.

6. Experiments with sphere shadows

The experiments were performed with the same ultrasonocardiograph USK 79/M in water with suspended talcum powder. This enabled us to obtain an inhomogeneous medium and thus to make the shadow visible. The spheres used first were made of stainless steel and the next of plasticine. The last ones made it possible to eliminate internal multiple reflexions which distorted completely the shadows. The plasticine spheres with the radii $a = 2$, 1 and 0.5 mm were easily detected with the echo method as well as steel spheres and even steel wires with the radii 0.25 and 0.05 mm perpendicular to their axis and situated parallel to the ultrasonic beam.

The shadow behind the plasticine sphere was very distinct only when the radius was equal to $a = 4\lambda = 2$ mm ($ka = 25$), while for $a = 2.5\ \lambda = 1.25$ mm ($ka = 16$) it was difficult to observe, although readily seen in the photograph (Fig. 5). The visibility of the shadow also depends on the ratio of the shadow radius to the ultrasonic beam radius, which in our case was ~ 0.3. White points in the right picture, near to the left shadow zone, are caused by greater talcum particles suspended in water.

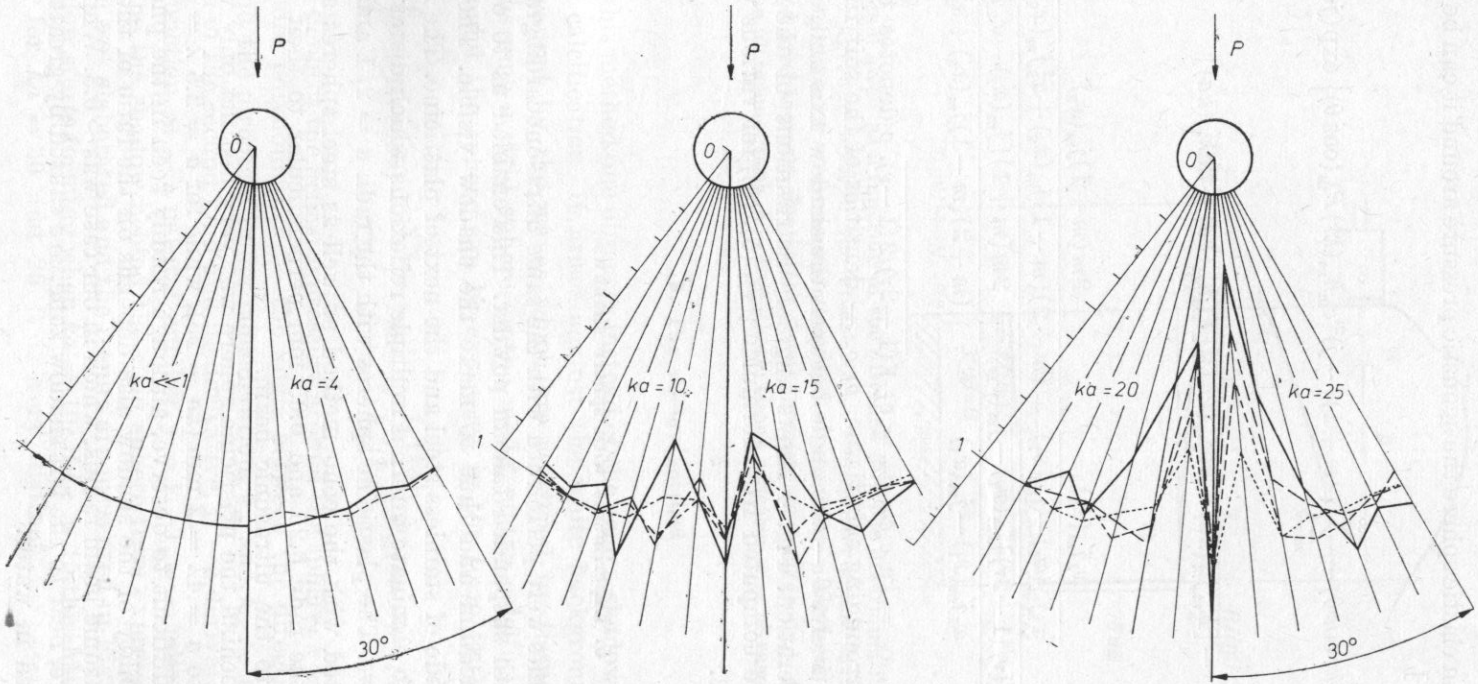

Fig. 3. The angular distribution of the acoustic pressure amplitude behind a rigid sphere. P — incident plane wave, a — radius of the sphere, r — distance from the sphere center, solid line — $r = 20\lambda$, long dashed line — $r = 40\lambda$, short dashed line — $r = 60\lambda$, dotted line — $r = 80\ \lambda$

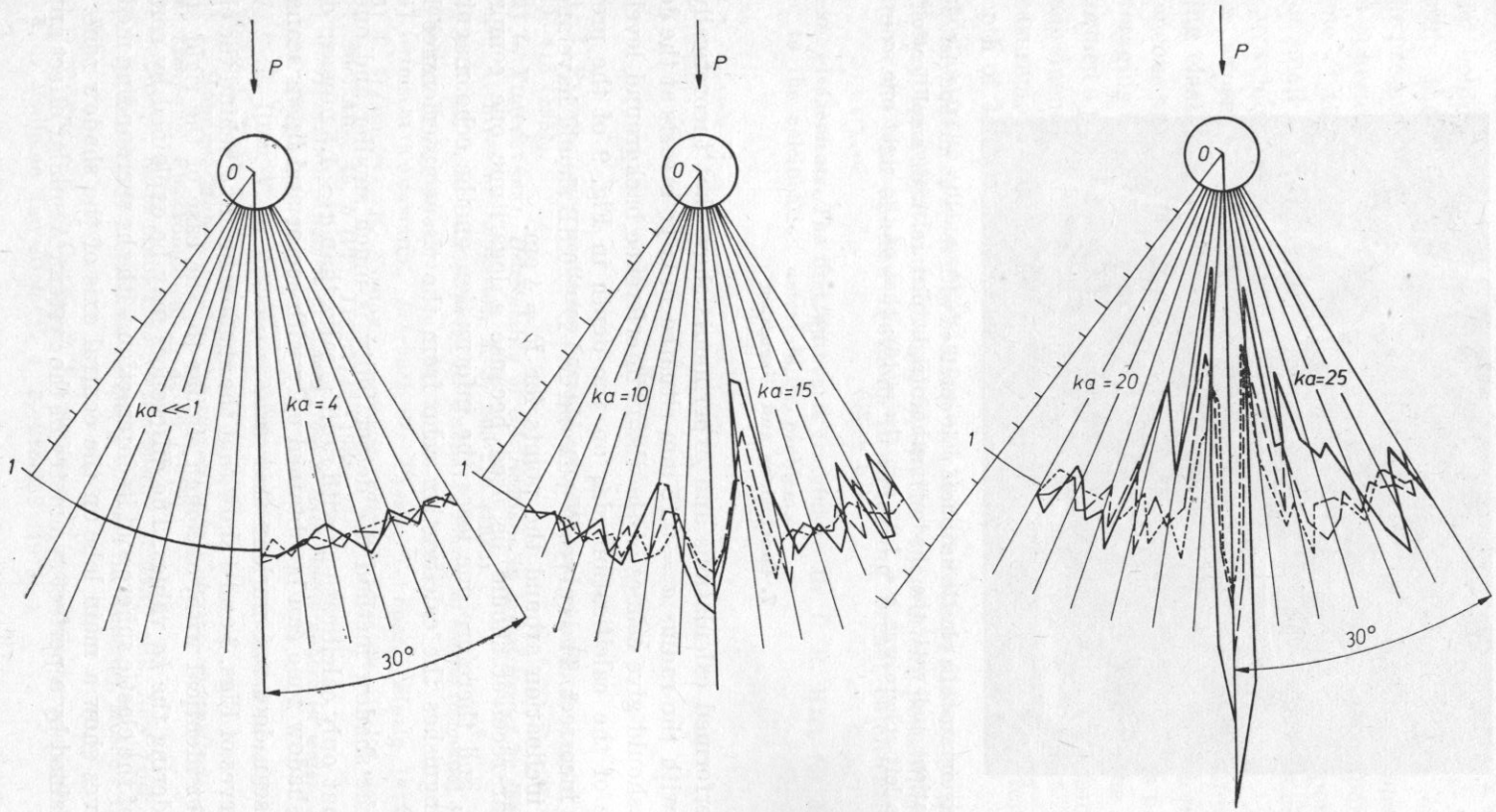

Fig. 4. The angular distribution of the acoustic pressure amplitude behind an elastic sphere (see Section 2) at the distance $r = 20\,\lambda$ (solid line), $r = 40\lambda$ (long dashed line) and $r = 60\lambda$ (short dashed line). Poisson ratio $\nu = 0.2$

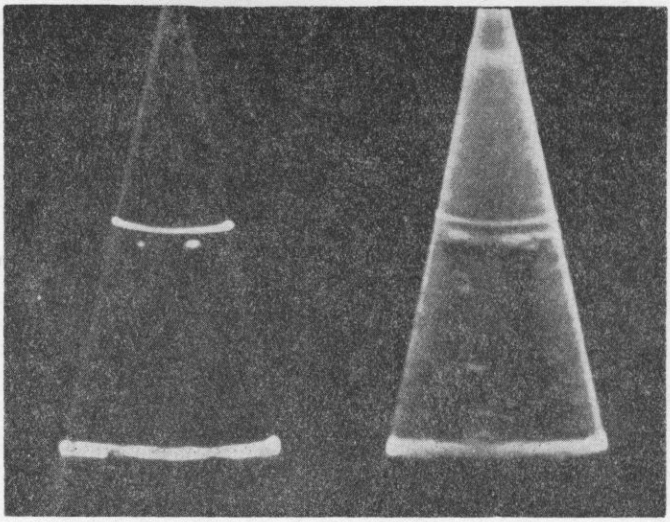

Fig. 5. Ultrasonograms of a plasticine sphere pair obtained with the echo method (left picture, low amplification) and with the shadow method (right picture, high amplification). The radius of the left sphere was $a = 1.25$ mm ($ka = 16$); that of the right one, $a = 2$ mm ($ka = 25$)

7. Conclusions and discussion

The performed calculations and experiments show that theoretically calcifications with the radius $a = 0.15$ mm situated in large breasts at the depths $R = 4$ cm, should give echoes of the tissue interference background level. The dependence of the calcification size on the depth in Fig. 9 of the previous paper [2] is incorrect. The curves $N+D$ and $N+D+20$ dB should have another shape and inclination around the points for $R = 4$ cm.

A linear receiver should be used because a logaritmic one compresses the signals, and therefore one loses the information on the echo magnitude, which distinguishes the calcification echo from the tissue interference background.

With the shadow method the detectability is much smaller and one can conclude that only calcifications with radii greater than $a \cong 1.5$ mm are detectable. The shadow zone can be obtained only with sector and linear scans, the compound scan does not work in this case.

The curves of Figs. 3 and 4 show that the shadow forming behind the elastic sphere is not identical with, although similar to, the case of the rigid sphere when considering the ka values. The differences may be explained by complex vibrations of the elastic sphere and its interaction with the surrounding medium. All the curves show a main lobe on the central axis of the shadow zone. This can be explained by a perfect symmetry of the system. A similar effect appears

in optics behind a circular screen where it is explained by means of Fresnel diffraction theory [4].

The present conclusions are based on a number of approximations which include a spherical shape of calcifications and their mechanical properties being the same as those of the skull bone. The steady-state analysis performed is valid for small calcifications; however, when the calcification size is comparable to the wavelength the obtained results are approximate.

Our experimental case did not correspond exactly to computed cases regarding elastic properties of the spheres. Also, the incident wave was not homogeneous and the ultrasonic beam scanned the spheres 25 times per second, thus averaging the shadow behind them. It was also assumed that the ultrasonic beam formed a parallel homogeneous wave, when a weak focusing beam was used in measurements of the tissue interference background.

Measurements of the tissue interference background were performed only at a depth of 4 cm.

It seems to the authors that in spite of the limitations discussed, the present estimation gives essential information on the theoretical possibilities of the ultrasonic echo and shadow methods in detecting breast calcifications.

Acknowledgements. The first author is grateful to Dr. C. R. HILL for drawing his attention to the calcification detectability problem.

References

[1] J. FARAN, *Sound scattering by solid cylinders and spheres,* J. Acoust. Soc. Am., **23**, 4, 405-418 (1951).

[2] L. FILIPCZYŃSKI, *Detectability of calcifications in breast tissues by the ultrasonic echo method,* Archives of Acoustics, **8**, 3, 203-220 (1983).

[3] L. FLAX, C. R. DRAGONETTE, H. UBERALL, *Theory of elastic resonance exitation by sound scattering,* J. Acoust. Soc. Am., **63**, 3, 723-731 (1978).

[4] Grimsehl TOMASCHEK, *Lehrbuch der Physik,* Teubner, Leipzig 1943, **II**, 589.

[5] T. HASEGAWA, K. YOSIOKA, *Acoustic radiation force on a solid elastic sphere,* J. Acoust. Soc. Am., **46**, 5 (P2), 1139-1143 (1969).

[6] R. HICKLING, *Analysis of echoes from a solid elastic sphere in water,* J. Acoust. Soc. Am., **34**, 1582-1592 (1962).

[7] C. R. HILL, V. R. MCCREADY, D. O. COSGROVE, *Ultrasound in tumor diagnosis,* Pitman Medical, Kent 1978.

[8] V. MENGES, *Mammographie, die zuvelässigste Untersuchungsmethode zur Brustkrebs-Früherkennung,* Electromedica, **2**, 42-49 (1979).

[9] O. MORSE, K. INGARD, *Theoretical acoustics,* McGraw Hill, New York 1968.

[10] S. N. RSHEVKIN, *Lectures on the theory of sound* (in Russian), Moscow University, Moscow 1980.

[11] D. N. WHITE, G. R. CURRY, R. J. STEVENSON, *The acoustic characteristic of the scull,* Ultrasound in Medicine and Biology, **4**, 3, 225-252 (1978).